INTERNATIONAL JOURNAL OF PHARMACEUTICAL, CHEMICAL AND BIOLOGICAL SCIENCES

Available online at www.ijpcbs.com

Research Article

NOVEL GRAPHENE-BASED REINFORCED HYDROXYAPATITE COMPOSITE COATINGS ON TITANIUM WITH ENHANCED ANTI-BACTERIAL, ANTI-CORROSIVE AND BIOCOMPATIBLE PROPERTIES FOR IMPROVED ORTHOPEDIC APPLICATIONS

N. Murugan, M. Chozhanathmisra, S. Sathishkumar, P. Karthikeyan and R. Rajavel*

Department of Chemistry, Periyar University, Salem - 636011, Tamilnadu, India.

ABSTRACT

A surface coating strategy encompassing the use of bioactive trace elements and reinforcing material will have significant influence on mechanical and osseointegration properties of bioceramic coated implants. Here, We attempted to mimic developed a minerals substituted and graphene oxide reinforced hydroxyapatite (Se,Mn-HAP/GO) composite coating on titanium (Ti) by electrodeposition which is a promising approach to produce bioimplants with better osseointegration capacity and improved mechanical property. Mechanical and biological studies were used to characterise the coatings. The composite coating on Ti was characterized by Fourier transform infrared spectroscopy (FTIR), X-ray diffraction (XRD), field emission scanning electron microscopy (FESEM). Also, the corrosion resistance of the coatings was evaluated by electrochemical techniques in simulated body fluid (SBF) solution. The *in vitro* cell-material interaction of the composite coating was observed with human osteosarcoma MG63 cells for cell viability at 1, 2 and 3 days of incubation. From the results we believe that the (Se,Mn-HAP/GO) composite coating on Ti could provide effective corrosion protection, enhanced bioactivity. Thus, composite coated Ti can serve as a potential candidate for orthopedic applications.

Keywords: Graphene oxide, reinforced hydroxyapatite, Mechanical, orthopedic applications.

1. INTRODUCTION

Biomaterials are artificial or natural materials, used in different parts of the human body to replace the lost or diseased organs and to restore their original form and function. In general biomaterial helps in improving the quality of life and longevity of human beings and has shown rapid growth to keep with the demands of an aging population. Pure titanium and its alloys are the most used biomaterials for fabrication of surgical implants due to their good mechanical properties, biocompatibility and resistance to corrosion[1-3] However, metallic surfaces are in general not adequately bioactive, and surface treatment is usually needed to enhance the bioactivity so as to improve osseointegration with bone tissues. It is important to heal in a short time; however the formation of new bone on the surface of implants needs a long time. In addition, implant products sometimes drop out from the bone and patients are forced to bear the burden of retreatment and its pain. To overcome the problems, an enhanced bioactive layer had to be developed over the surface of the metallic implants to promote high comprehensive bone growth (osteoconductivity). In view of these, Ti implants are commonly coated with hydroxyapatite (Ca_{10} $(PO_4)_6$ $(OH)_2$, a bioceramic material with chemical and crystallographic similarity to that of natural apatite in bones and

has been currently used in hard tissue engineering for bone repair or regeneration. This bioactive coating on Ti implants improves the integration between the implants and bone tissues. However, the inferior wear resistance and fracture toughness of HAP cannot match the mechanical behavior of natural bone and would hinder its clinical application in major load-bearing devices as coating materials[4-10].

However, intrinsic brittleness, low wear resistance, and low fracture toughness still limit the use of HAp in load-bearing and long-term implant applications[11-14]. Mechanical performance of HAP can be improved by incorporating second phase reinforcements such as ceramics and polymers. One of the most common approaches to overcome this weakness and to provide better corrosion resistance, incorporation of reinforcing materials like CNTs, TiO_2, and ZrO_2 is followed As an ideal reinforcing[15-20]. Therefore, the hybridization of HAP and GO will make full use of the advantages of both GO and HAP and a hybrid composite with good mechanical properties and favorable cell responses is expected when GO and HAp are simultaneously used as dual reinforcements. Furthermore, GO can facilitate the interfacial interactions with the matrixes owing to its abundant oxygen functional groups (e.g., hydroxyl, epoxide, and carboxyl groups) and has been increasingly believed to be an ideal reinforcement for composites. have been used to form composites with GO and improved mechanical properties, cell attachment, proliferation, and cell growth have been demonstrated[21-24].

Furthermore, the HAP based bioceramic material might be improved by the addition of bioactive ions to improve the biological properties of the implants applications[25-27]. In particular, the positive effect of bioactive ions such as magnesium (Mg^{2+}), zinc (Zn^{2+}), manganese (Mn^{2+}), strontium (Sr^{2+}), silver (Ag^{2+}), silicon (Si^{2+}), etc., in HAP based coatings on metallic substrates has been reported[28-37]. The incorporation of specific elements can then be used to tune the biological properties of the apatite.

Manganese is a trace element which is essential for the growth and development of bones. The radius of manganese ions (0.99 Å) is very close to that of calcium (0.90 Å), which enables Mn ion to enter osteoblasts through calcium ions channels. Manganese influences bone metabolism by regulating the osteoblast differentiation and bone resorption. Thus, Mn has been substituted in HAP to improve the biocompatibility and osteoblast differentiation. The presence of Mn in calcium phosphate can also improve the production of osteocalcin in osteoblasts, even more effectively than strontium and magnesium. In order to enhance the bone bonding ability and to promote osteoblast differentiation, a substituent (Mn) is introduced into the coating[38-42].

Until recently, selenium was considered as a essential and unique trace element that plays a crucial role in health and disease. Meanwhile, Se has also been reported as an efficient anticancer agent. Se inhibited the growth of cancerous osteoblasts and promoted the proliferation of healthy osteoblasts. Numerous studies indicate that a selenium deficiency may cause an inhibition of bone growth in rats as well as a severe reduction of bone strength. Apart from the therapeutic properties mentioned, Se also enhances the corrosion resistance of metals and alloys. Moreover, it is reported that Se substituted HAP is potentially a promising bone graft material. Although, the minerals substituted biomaterial is capable for improving various biological property[43-52].

Hence, the main aim of our work is the development of Se,Mn-HAP/GO composite coating on Ti. The Se,Mn-HAP/GO composite material may be an ideal biocomposite for orthopedic implantation because of its improved strength, hardness, and toughness where compared to the pure HAP . In the present work, Se,Mn-HAP/GO composite coated Ti improves the corrosion resistance, mechanical and biological properties.

A number of coating technologies are available for the development of bioceramic coatings and among them the electrochemical deposition has unique advantages due to its relatively low deposition temperature, process simplicity, capability of forming a uniform coating on porous substrates (or) complex shapes of substs and the availability and low cost of equipments[53-56]. To the best of our knowledge, there are no reports on the electrodeposition of leaf like Se,Mn-HAP/GO composite coating on Ti. Hence we propose that the Se,Mn-HAP/GO composite coating Ti could improve the corrosion resistance, proliferation of healthy osteoblasts and inhibit the growth behaviors of bacteria cells.

2. MATERIALS AND METHODS

2.1 Chemicals

All chemicals were of analytical grade and used without further purification throughout the experiments. The chemicals used for the GO sulphuric acid (H_2SO_4). For the Mn,Se-HAP

synthesis, calcium nitrate tetrahydrate ($Ca(NO_3)_2$ $4H_2O$), manganese nitrate hexahydrate ($Mn(NO_3)_2$ $6H_2O$), sodium selenite $Na_2SeO_3{\cdot}5H_2O$, diammonium hydrogen phosphate ($(NH_4)_2HPO_4$) and ammonia solution (NH_4OH) were used. Deionized water and ethanol were employed as the solvents throughout the experiment.

2.2 Specimen preparation

The pure titanium specimens (99.99%) of the size 10 × 10 × 3 mm were cut and embedded in epoxy resin, leaving area of 1 cm^2 for exposure to the solution. Prior to electrodeposition, the samples were abraded with different grades of SiC emery papers from 400 to 1200 grit and washed with distilled water, degreased with acetone, then dried at room temperature. all the samples were ultrasonically cleaned in 100% acetone for 10 min, in order to remove any surface residues. All received a final rinse in deionized (DI) water and then dried immediately in flowing air. Clean Ti placed under UV radiation for 1 h on each side for sterilization and then used for further studies.

2.3 Preparation of Se,Mn-HAP electrolyte

Analytical grade $Ca(NO_3)_2$ $4H_2O$, $(Mn(NO_3)_2$ $6H_2O)$ and $Na_2SeO_3{\cdot}5H_2O$ were dissolved in deionized water separately and the solutions were mixed in the ratio of 8:1:1, respectively. The $(NH_4)_2HPO_4$ was dissolved in deionized water and both the solutions were mixed to produce the target (Ca+ Mn)/P+Se ratio of 1.67. The electrolyte was prepared in the pH of the electrolyte was maintained to 4.7 at 28 °C using thermostat. The electrolyte was magnetically stirred for 4h at a speed of 180 rpm to maintain uniform concentration.

2.3.1 Preparation of Se,Mn-HAP/GO electrolyte

The modified Hummers method was utilized to graphene oxide (GO) was prepared by using graphite powder was applied to oxidize graphite for the synthesis of GO. As described in the literature.[57] The electrolyte was prepared by mixing a solution containing $Ca(NO_3)_2$ $4H_2O$, $(Mn(NO_3)_2$ $6H_2O)$,$Na_2SeO_3{\cdot}5H_2O$ and $(NH_4)_2HPO_4$ under constant stirring during 3 h. The different concentration (0–3 wt.%) of the grapheme oxide were gradually added to the above solution and the pH was adjusted to 4.7 using NaOH or HCl.

2.4 Electrodeposition of Se,Mn-HAP and Se,Mn-HAP/GO on Ti

The electrodeposition of M-HAP, Mn,Se-HAP/ GO was performed in a common three electrode configuration where Ti specimens served as a working electrode, platinum and saturated calomel electrode as counter electrode and reference electrodes, respectively. The deposition was carried out in potentiostatic mode by applying a potential of 1 V vs. SCE during 1 h using an electrochemical system CHI 760C (CH instruments, USA).After the electrodeposition, coated specimens were removed from the electrolyte and were gently rinsed with deionized water, and then dried for 24 h. Finally, all the samples were sterilized in an autoclave and stored in desiccators at room temperature.

2.5 Characterization of coatings

2.5.1 Phase structure and morphological characterization

The functional groups present in the coatings were identified by Fourier transform infrared spectroscopy (FTIR, Bruker Tensor 27) over the wave length range of 4000-400 cm^{-1}.

The phase composition of the as-developed coatings was investigated by X-ray diffraction (XRD, Bruker D8 Advance diffractometer) in the 2θ range of 10-80° at a scan rate of 0.02°. Morphological investigations of the coatings were performed using a field-emission scanning electron microscope Hitachi (FE-SEM S4800) operating at an accelerating voltage of 30.0 kV.

2.5.2 Mechanical characterization

The adhesion strength of the coating is of utmost importance for the implant to function properly in load bearing applications. The adhesion strength of the HAP, Se,Mn-HAP, Se,Mn-HAP/GO composite coatings on Ti implant was carried out by the pull-out test according to the American Society for Testing Materials (ASTM) international standard F1044 with at least five measurements for each experiment. Prior to the adhesion test all the coated samples were cured in an oven at 150 ºC for 1 h and the fixtures were subjected to pull-out test using a universal testing machine (Model 5569, Instron) at a crosshead speed of 1 mm min^{-1}.

2.6 Electrochemical evaluation of the composite coatings

The electrochemical experiments were carried out through electrochemical impedance spectroscopy (EIS) in under simulated body fluid [SBF] conditions 7.4 pH and 37 °C solution.[Table1] The electrochemical measurements were performed with a standard three-electrode cell arrangement using the CHI 760 electrochemical workstation (USA), consisting of a saturated calomel electrode

(SCE), Ti and platinum electrodes as the reference, working and counter electrodes, respectively. The EIS experiments were performed in the frequency range of 10^{-1} Hz to 100 kHz with perturbation amplitude of 5 mV. All the measured potential values are related to the SCE and all the electrochemical parameters are normalized with respect to the area of the Ti electrode (1 cm^2). The obtained electrochemical data were recorded using internally available software and the corrosion tests were repeated at least three times to ensure reliability and reproducibility and the results were found to be reproducible.

2.7 Antibacterial activity

The in vitro antibacterial activity of the samples was tested against bacterial strains E. coli by the agar disc diffusion method. The inoculua of the selected bacterial species were prepared from the fresh overnight the cultures (Tripton soy broth with 0.6% yeast extract- Torlak, Serbia) that were incubated at 37 ºC with constant stirring and were then used for the diffusion studies. The diffusion technique was carried out by pouring agar into petri dishes to form 4 mm thick layers and adding dense inoculum of the test organisms of bacterial strains in order to obtain better growth. Petri plates were left for 10 min in the laminar air flow and after that, discs (6 mm) were prepared from Whatman no:3 filter paper, immersed into different volumes of (25, 50, 75, 100, 125 mL) composite coated samples, placed at equal distances and then incubated at 37 ˚C for overnight in a bacteriological incubator. The results were obtained by measuring the width of zone of inhibition (mm) around the disc which was produced by the coating samples against the bacterial strains.

2.8 In vitro cytotoxicity

Human osteosarcoma MG63 osteoblast-like cells (HOS MG63, ATCC CRL-1427TM) were purchased from National Centre for Cell Sciences (NCCS), Pune, India, and then cultured in standard culture medium (Dulbecco's Modified Eagle Medium (DMEM, GIBCO)), which consisted of a minimal essential medium, supplemented with 10% fetal bovine serum (FBS), and 1% non-essential amino acids (GIBCO). The minimal essential medium was renewed for every two days and then the cultures were maintained in a humidified atmosphere of 5% CO_2, at 37 °C. The osteoblast cultures were separated from the culture flask by incubation with 0.1% trypsin and 0.1% ethylene diamine tetraacetic acid (EDTA) for about 5 min. The viability of HOS MG63 cells colonizing the samples (Se,Mn-HAP/GO composite coatings) were evaluated using MTT (3-(4,5-dimetyl-2-tiazolyl)-2,5-diphenyl-2Htetrazolium bromide) assay. To determine the cytotoxicity of the samples at different conditions, HOS MG63 cells were seeded in 12-well plates at 104 cells/ml in a humidified 5% CO_2 atmosphere. After 24 h of incubation, MTT solution (in 1 ml serum free medium) was added and then incubated for 4 h at 37 °C in a humidified 5% CO_2 atmosphere. The solution was removed and dimethyl sulfoxide was added to it, and the plate was shaken for 15 min before measuring absorbance at 570 nm (the reference value was 690 nm) on an ELISA microplate reader and then % cell viability was calculated with respect to control as follows,

% Cell viability = [A] Test/[A] Control X 100.

3. RESULTS AND DISCUSSION

3.1 Surface characterization of the (Se,Mn-HAP/GO composite) coatings

3.1.1 FT-IR analysis

The FT-IR analysis of Se,Mn-HAP/GO composite coated Ti was carried out and the corresponding spectra are shownin Fig.1 The FT-IR spectrum of the Se,Mn-HAP/GO composite coating is shown in Fig. 1. which shows the characteristic peaks corresponding to phosphate (PO_4^{3-}) groups (985 cm^{-1}, 1150 cm^{-1}, 550 cm^{-1} and 605 cm^{-1}) and hydroxyl (OH^-) groups (stretching vibration at 3580 cm^{-1} and libration mode at 650 cm^{-1}), respectively. Additionally, the peaks due to the stretching and bending modes of adsorbed water (H_2O) molecules can be seen at 3480 cm^{-1}.The peak assignments are in accordance with the literature data. Grapheme oxide shows typical absorption bands at 1620 cm^{-1} and 1045 cm^{-1} which are assigned to, C=C stretching mode and C-O stretching vibration respeatively. As a result, the spectrum (Fig. 1) strongly supports All these peaks support for the formation of Se,Mn-HAP/GO composite coating on Ti.

3.1.2 XRD analysis

The XRD patterns of Se,Mn-HAP/GO composite coated Ti are shown in Fig. 2. The diffraction peak values (2θ) of 25.9˚, 31.5˚, 32.4˚, 33.2˚, 46.7˚, 49.5˚ and 53˚ were assigned to HAP (Fig. 2). All these diffraction peaks confirm the presence of HAP and agree well with the International Centre for Diffraction Data (ICDD card no. 09-0432). Fig. 2depicts the XRD pattern obtained for the Se,Mn-HAP/GO composite coated Ti which is in good

agreement with the standard data for HAP. The remaining peaks observed at 2θ values of 36.3˚, 47.5˚ and 56.4˚ correspond to GO. This evidences the formation of Se,Mn-HAP/ GO composite coating on Ti.

3.1.3 Morphological characterization

Fig. 3 (a–d) represents the SEM micrographs at different concentrations of GO (0, 1, 2and 3 wt %) in the Se,Mn-HAP/GO composite coated titanium. The coating structure exhibited different crystal morphology at different concentrations of GO in the Se,Mn-HAP/GO composite. Fig. 3(a) shows a uniform porous distribution of Se,Mn-HAP matrix with the existence of on the surface of titanium. The coating morphology of 1 wt.% Se,Mn-HAP/GO shows the formation of grow into flower-like structure (Fig. 3b). In the addition of 2 wt.% GO, slanting and perpendicular flake like porous may develop covering the entire surface of titanium (Fig. 3c). On further concentration increases of GO to 3 wt.%, these flake-like structure grows outwardly and disorderly forming macro porous structure over the surface that paves the way for the detachment of the composite coating from the surface of titanium (Fig. 3d). Moreover, the morphology of Se,Mn-HAP/GO coating on titanium revealed a rough surface with a uniformly distributed microstructure. It may be better to have the porous flake like structured coating for bone growth, since the inorganic apatite in the bone has plate shaped morphology.

3.1.4 Mechanical characterization of the Se,Mn-HAP/GO composite coatings

Adhesion strength of the coating on the metallic implants is one of the important properties for *in vivo* implantation. Here, the adhesion strength of the HAP, Se,Mn-HAP, and Se,Mn-HAP/GO (2wt.%) composite coatings on titanium (Fig.4) was evaluated.

The adhesion strength of the HAP coated titanium (17.6±0.4 MPa) , Se,Mn-HAP (20.5±0.6 MPa) and Se,Mn-HAP/GO (2wt.%) (27.8 ±0.5 MPa) was higher than that of pure HAP and Se,Mn-HAP composite coated titanium, respectively. This improved adhesion strength of the as-formed composite coating will make it suitable for load bearing applications.

3.2 Electrochemical Impedance Spectroscopic Studies

The impedance spectra for uncoated, Se,Mn-HAP and Se,Mn-HAP/GO composite coated titanium specimens in the SBF solution. The experimental data represented as Nyquist plots (Fig. 5) For the Se,Mn-HAP coated titanium, the Rp value was found to be 190.4 kΩ cm^2 which showed higher corrosion resistance than the uncoated titanium (Rp = 52.5 kΩ cm^2). The Rp values of titanium coated with the Se,Mn-HAP/GO composite containing concentrations of GO (2 wt.%) are 225 kΩ cm^2, respectively. Thus, the higher impedance values of the 2 wt.% Se,Mn-HAP/GO (2 wt.%) composite coating suggest that the coating hinders the ion diffusion process and thereby enhance the corrosion resistance of titanium. From this study it is well evident that, Se,Mn-HAP/GO serves as a protective barrier layer between the composite coated titanium with higher corrosion resistance can serve as a potential material for *in vivo* implantation (load bearing applications).

3.3 Biological characterization of the Se,Mn-HAP/GO composite coatings

3.3.1 Antibacterial activity

E. coli are the general bacteria's that are found in the contaminated wound. The as developed, control, Se,Mn-HAP and Se,Mn-HAP/GO composite coatings were tested against E. coli stains at different concentrations like 25, 50, 75, 100 and 125 µg/ml and compared with control. Antibacterial results obtained for the coatings are presented in Fig.6 shows that the Se,Mn-HAP/GO composite coating gave higher antibacterial activity against Gram-negative bacteria because of the substitution of Se in Mn-HAP that can react with the nuclear content of bacteria and destroy them Se,Mn-HAP/GO composite coatings showed excellent anti-bacterial activity. Fig.6 The measured inhibition zones for the Se,Mn-HAP/GO composite coating was found to be 7.5, 9.8, 13.9, 16, and 21.5 mm for *E. coli* respectively. From the results it is well evident that the Se,Mn-HAP/GO composite coating not only retards the bacterial adhesion, but also effectively kills the adhered bacteria suggesting effective and long lasting antibacterial activity against *E. coli* .

3.3.2 In vitro cytotoxicity assessment of composite against human osteoblast cells

The cytotoxicity assay was used to determine the viability of human osteoblast cells on the (Se,Mn-HAP/GO) composite coating cultured for 1, 2 and 3 days. The percentage cell viability of composite coating was calculated with respect to the for 1, 2 and 3 days and the results are shown as bar diagram in Fig.7 From the Fig.8 it is well evident that, as the days of incubation is increased, the % cell viability also increased which is in good

agreement with the fluorescence microscopic images as shown in Fig. 8 (a-c). The composite coatings exhibited a substantial cell viability which is similar to that of the (Fig. 8 (a)). At day 1, the cells distributed evenly and spread on the coated sample. On day 2, the cells got spread better on the surfaces when compared to that on day 1. Almost no dead cell can be observed from the samples. As the incubation was increased to 3 days, the number of cells also increased and fully covered on surface. This is an indication that the composite (Se,Mn-HAP/GO) coating has nearly no cytotoxicity and indeed support cell proliferation. The composite coatings at 3 days of culture (Fig. 8(c)) showed the presence of more viable cells which evidence that the biocompatibility of the composite is not affected by the presence of mineral ions Se and Mn in the coating. It is also evident that. Does not affect the bioactivity of the composite coating. Thus, the MTT assay test clearly shows that the composite of Se,Mn-HAP/GO composite coating extensively increased the viability of cells (96.5%) which is favorable for orthopedic applications.

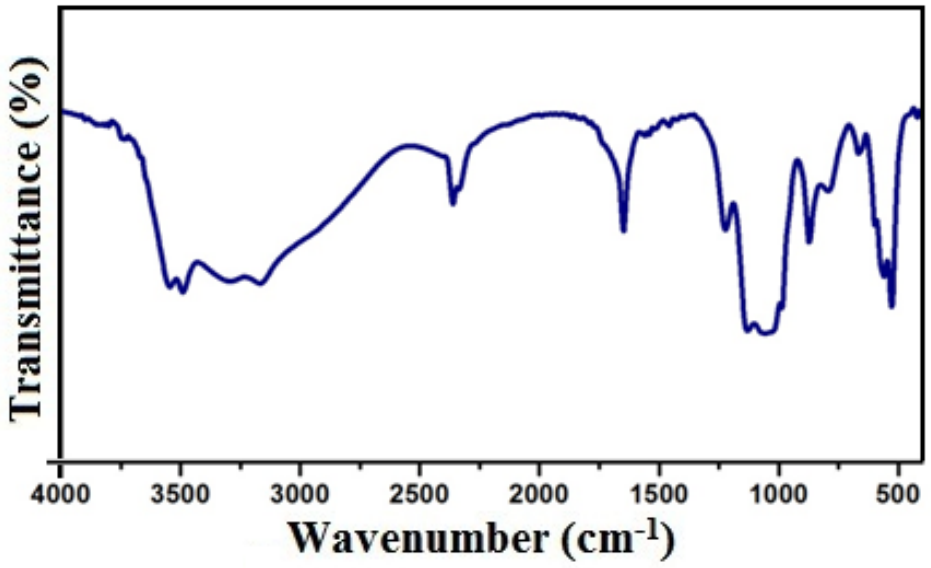

Fig. 1: FT-IR spectra of Se,Mn-HAP/GO composite coated titanium

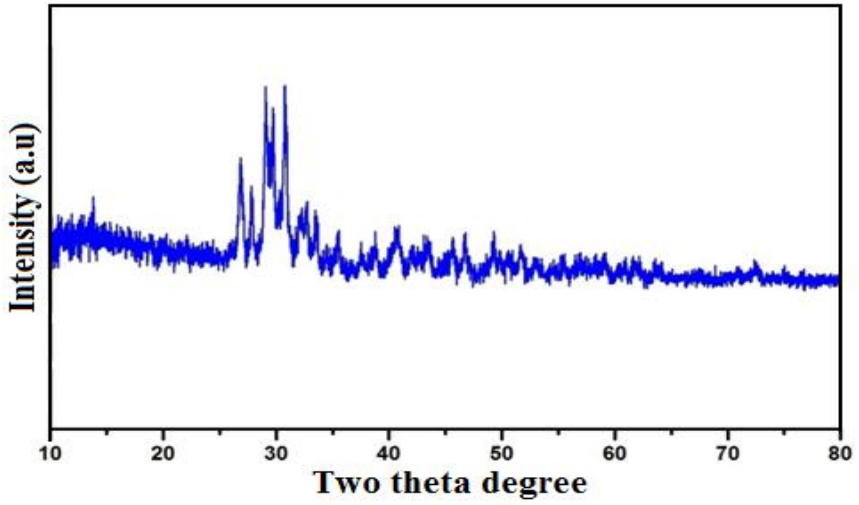

Fig. 2: XRD patterns of Se,Mn-HAP/GO composite coated titanium

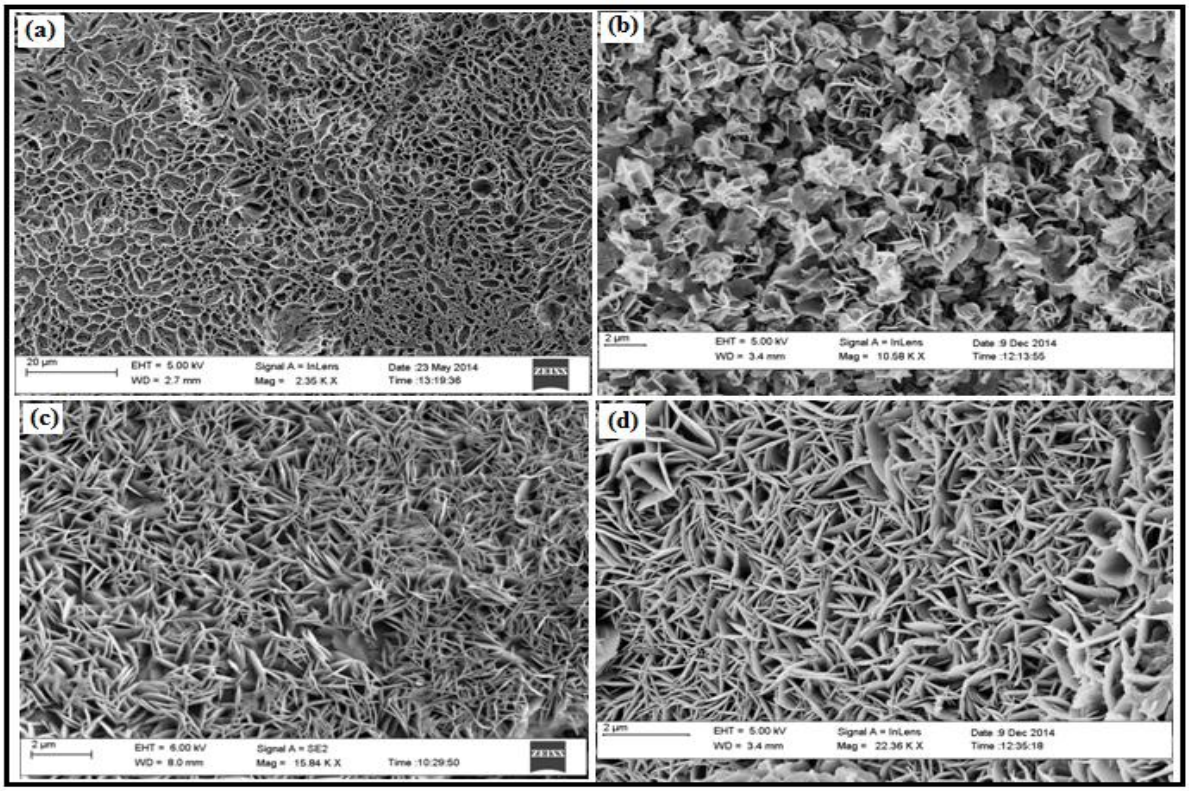

Fig. 3: FESEM images at different concentrations of GO in the Se,Mn-HAP/GO composite coating on titanium: (a) Se,Mn-HAP (b) Se,Mn-HAP/GO 1 wt.%, (c) Se,Mn-HAP/GO 2 wt.%, and (d) Se,Mn-HAP/GO 3 wt.%, coating on titanium

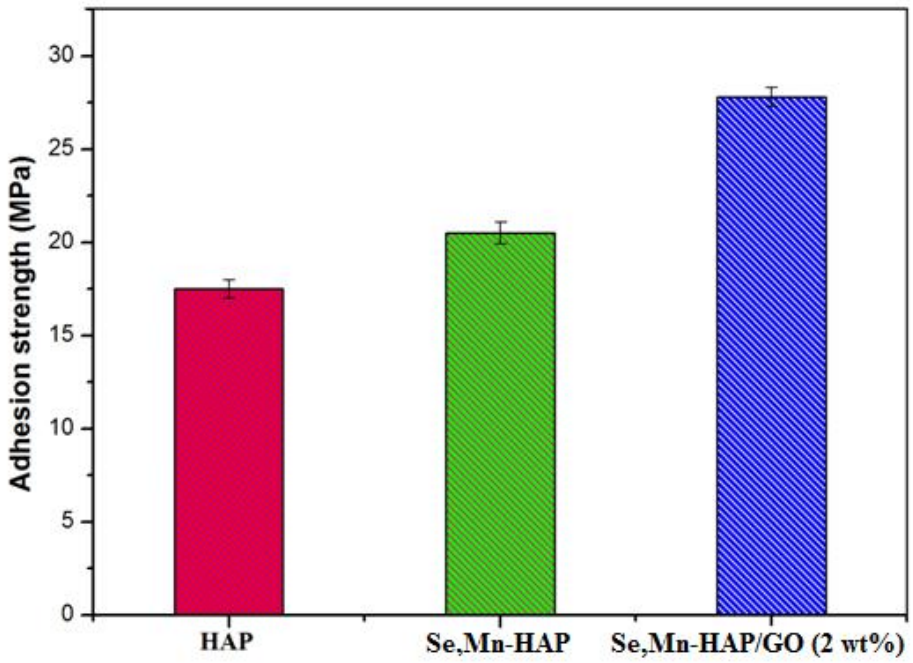

Fig. 4: Adhesion strength of HAP, Se,Mn-HAP, and Se,Mn-HAP/GO 2 wt.%, composite coated Ti

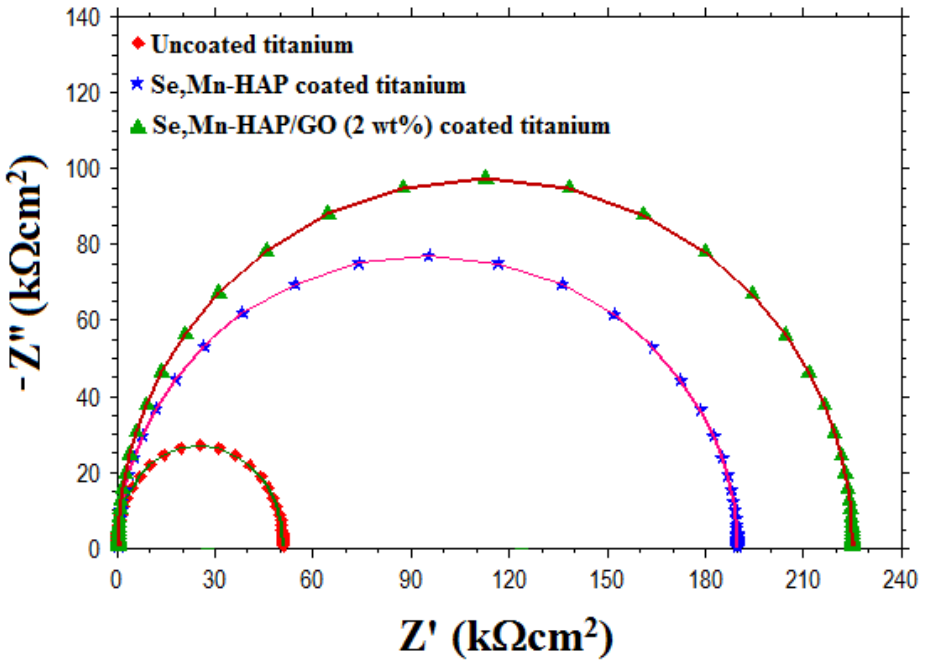

Fig. 5: Nyquist plots for uncoated, Se,Mn-HAP, and Se,Mn-HAP/GO 2 wt.%, composite coated titanium in SBF solution

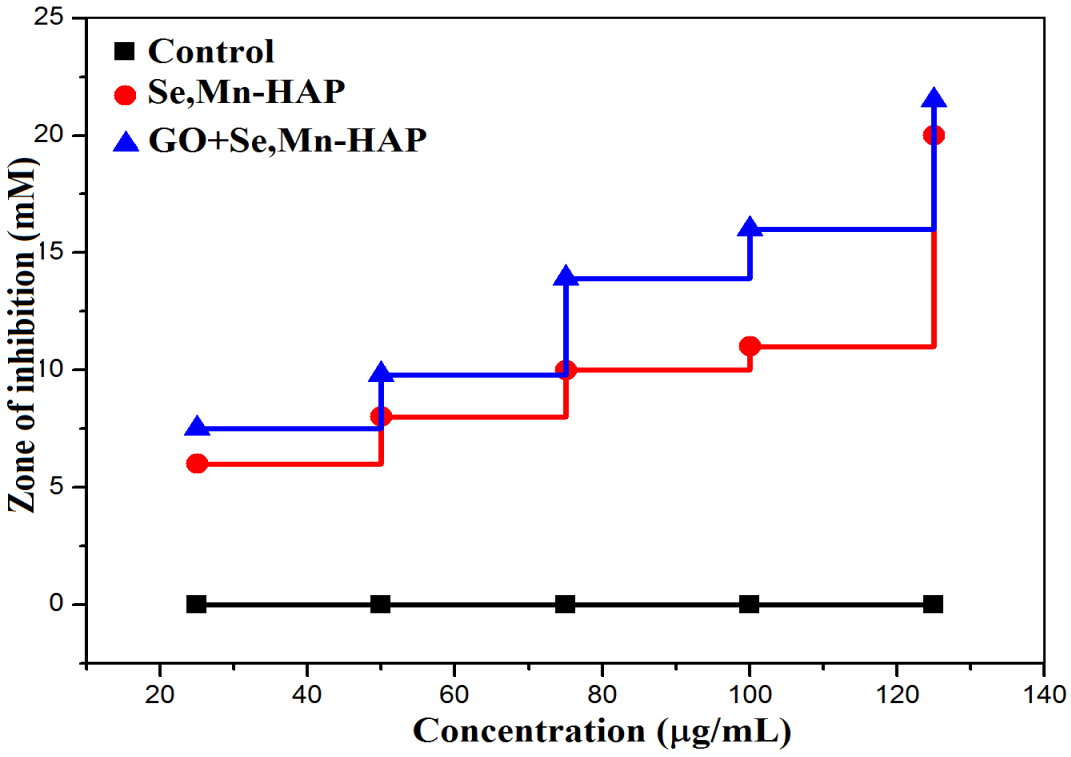

Fig. 6: Antibacterial activity of control, Se,Mn-HAP and Se,Mn-HAP/GO (2 wt%), composite coated samples with different concentrations of 25, 50, 75, 100, and 125 against *E. coli* for the zone of inhibition

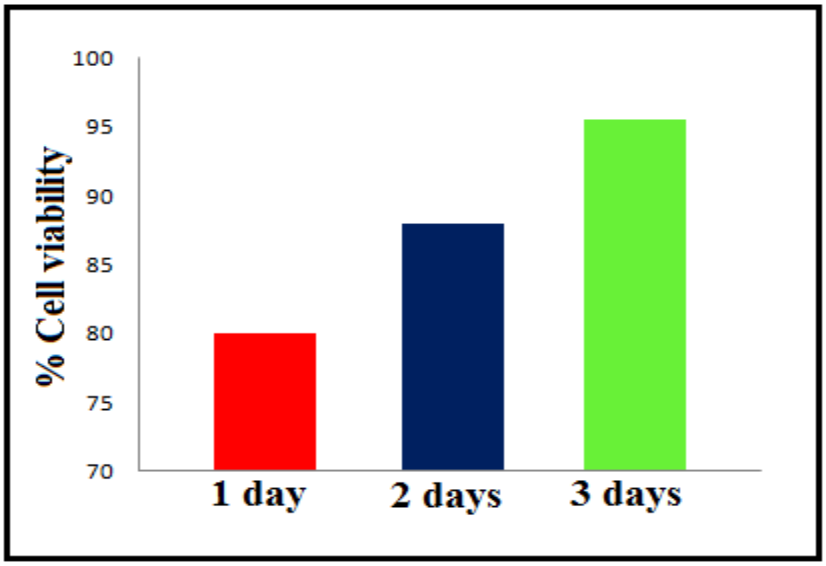

Fig. 7: Bar diagram showing the % viability of human osteoblast cells on Se,Mn-HAP/GO (2 wt%) composite coated titanium at 1, 2 and 3 days of incubation

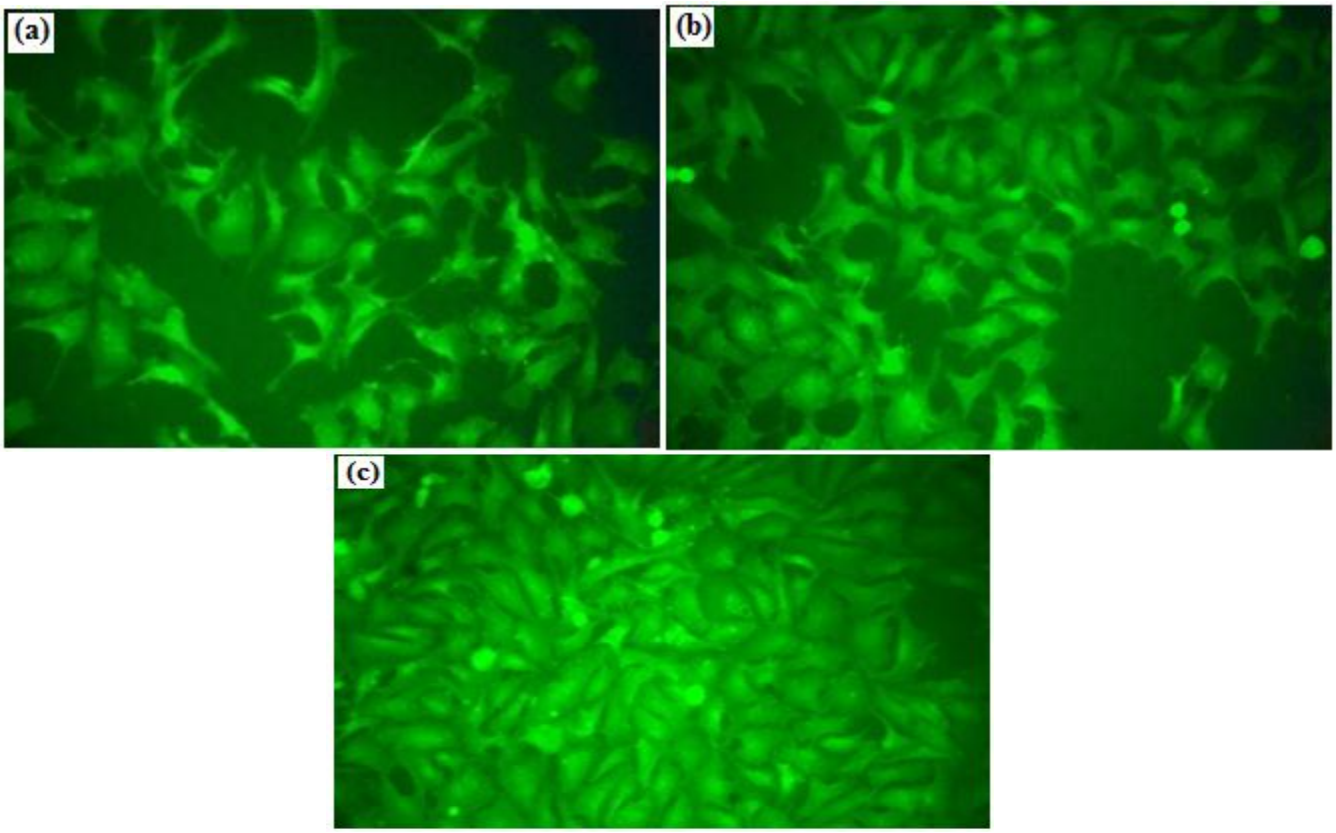

Fig. 8: Optical microscopic images showing the % viability of human osteoblast cells on Se,Mn-HAP/GO (2 wt%) composite coated titanium (a, b, c) at 1, 2 and 3 days of incubation

Table 1: Ionic composition of human blood plasma and SBF

Ions	Na^+	K^+	Ca^{2+}	Mg^{2+}	Cl^-	HCO_3^-	HPO_4^{2-}	SO_4^{2-}
Human Blood Plasma (mM)	142	5	2.5	1.5	103	27	1	0.5
SBF (mM)	142	5	2.5	1.5	147.8	4.2	1	0.5

4. CONCLUSIONS

In this paper, we have demonstrated the successful electrodeposition of Se,Mn-HAP/GO composite coatings on Ti. Having investigated the corrosion protection performance of all the as formed coatings, we found that the composite coating plays an effective role in improving the bioresistivity of Ti. This study also identified that the present of selenium and manganese in composite coating inhibited the antimicrobial functions, while still promoting the healthy osteoblast functions. All these results supports that the Se,Mn-HAP/GO composite coated Ti can be a promising implant material with multi-functional properties like enhanced corrosion resistance, mechanical, biocompatible and anti-bacterial properties. Composite coated Ti can be a promising candidate for orthopedic applications.

ACKNOWLEDGEMENTS

The authors are very grateful to our Supervisor for his encouragement and support.

REFERENCES

1. Z. Cai, H.Nakajima, M.Wold, A.Berglund, M.Bergman, and T.Okabe, Biomaterials, 1999 20, 183–190.
2. J. Cizek, K. A. Khor and Z. Prochazka, Mater. Sci. Eng., C, 2007, 27, 340-344.
3. P. Li, and P. Ducheyne, J. Biomed. Mater. Res., 1998, 41, 341–348.
4. C. G. Ambrose and T. O. Clanton, Ann. Biomed. Eng., 2004, 32, 171-177.
5. X.M. Li, Q.L. Feng, W.J. Wang and F.Z. Cui, J. Biomed. Mater. Res., 2006, 77B, 219–226.
6. T.M. Sridhar, U. Kamachi Mudali, and M. Subbaiyan, Corros. Sci., 2003, 45, 237–252.
7. X.H. Liu, X.M. Li, Y.B. Fan, G.P. Zhang, D.M. Li, W. Dong, Z.Y. Sha, X.G. Yu, Q.L. Feng, F.Z. Cui and F. Watari, J. Biomed. Mater. Res., 2010, 94B, 44–52.
8. X.M. Li, Q.L. Feng, Y.F. Jiao and F.Z. Cui, Polym. Int., 2005, 54, 1034–1040.
9. L Fang, Y Leng and P Gao. Biomaterials 2006;27, 3701–3707.
10. H. Yoshikawa and A. Myoui, J. Artif. Organ. 2005, 8, 131-136.
11. L. Fang, Y. Leng and P. Gao, Biomaterials, 2006, 27, 3701–3707.
12. Wu MY, Wang QY, Liu XQ, Liu HQ. Carbon, 2013, 35, 335–345.
13. Y. Gu, K. Khor, and P. Cheang, Biomaterials, 2004, 25, 4127–4134.
14. L.G. Yu, K. Khor, H. Li, and P.Cheang, Biomaterials, 2003, 24, 2695–2705.
15. T.M. Sridhar, U. Kamachi Mudali, and M. Subbaiyan, Corros. Sci., 2003, 45, 2337–2359.
16. X.H. Chen, C.S. Chen, H.N. Xiao, F.Q. Cheng, G. Zhang, and G.J. Yi, Surf. Coat. Technol., 2005, 191, 351–356.
17. B.M. Praveen, T.V. Venkatesha, Y. Arthoba Naik, K. Prashantha, Surf. Coat. Technol., 2007, 201, 5836–5842.
18. N. Ignjatovi, S. Tomi, M. Daki, M. Miljkovi, M. Plavsi, and D. Uskokovi, Biomaterials, 1999, 20, 809–816.
19. A. Bigi, E. Boanini, S. Panzavolta, and N. Roveri, Biomacromolecules, 2000, 1, 752–756.
20. J.D. Hartgerink, E. Beniash, and S.I. Stupp, Science, 2001, 294, 1684–1688.
21. D. Li, M. B. Muller, S. Gilje, R. B. Kaner and G. G. Wallace, Nat. Nanotechnol., 2008, 3, 101-105.
22. K. Yang, S. Zhang, G. Zhang, X. Sun, S. T. Lee and Z. Liu, Nano. Lett., 2010, 10, 3318-3323.
23. J. Zhu, H.M. Wong, W.K. Yeung, S.C.Tjong Adv. Eng. Mater., 2011, 13, 336–341.
24. Y. Liu, J. Huang, H.Li J. Mater. Chem B., 2013, 1, 1826–1834.
25. E. Boanini, M. Gazzano, A.Bigi, Acta. Biomater., 2010, 6, 1882–1894.
26. Y. Tang, H.F. Chappell, M.T. Dove, R.J. Reeder, Y.J.Lee, Biomaterials, 2009, 30, 2864–2872.
27. I. Cacciotti, A. Bianco, M. Lombardi, L. Montanaro, J. Eur. Ceram. Soc., 2009, 29, 2969–2978.
28. L. Obadia, P. Deniard, B. Alonso, T. Rouillon, S. Jobic and J. Guicheux, Chem. Mater., 2006, 18, 1425–1433.
29. A. Rawal, X. Wei, M. Akinc and K. S. Rohr, Chem. Mater., 2008, 20, 2583–2591.

30. A. A. Belik, F. Izumi, S. Y. Stefanovich, A. P. Malakho, B. I. Lazoryak and I. A. Leonidov, Chem. Mater., 2002, 14, 3197–3205.
31. R. Z. LeGeros, J. Dent. Res., 1974, 53, 45–50.
32. A. Bigi, E. Foresti, M. Gandol, M. Gazzano and N. Roveri, J. Inorg. Biochem., 1997, 66, 259–265.
33. O. Gunduz, L. S. Ozyegin, S. Dorozhkin, O. Meydanoglu, N. Eruslu and S. Kayali, Eng. Mater., 2009, 8, 396–398.
34. S. Kannan, S. Pina and J. M. F. Ferreira, J. Am. Ceram. Soc., 2006, 89, 3277–3280.
35. M. V. Regi and J. M. G. Calbet, Prog. Solid. State .Chem., 2004, 32, 1–31.
36. S. V. Dorozhkin and M. Epple, Angew. Chem., Int. Ed., 2002, 41, 3130–3146.
37. S. Kalita, S. Bose, H. Hosick and A. Bandyopadhyay, Biomaterials, 2004, 25, 2331–2339.
38. B. Bracci, P. Torricelli, S. Panzavolta, E. Boanini, R. Giardino, and A. Bigi. J. Inorg. Biochem., 2009, 103, 1666–1674.
39. F. Sima, G. Socol, E. Axente, I.N. Mihailescu, L. Zdrentu, S.M. Petrescu, and I.Mayer, Appl. Surf. Sci., 2007, 254, 1155–1159.
40. A.S. Hazell, P. Desjardins, and R.F.Butterworth, Neuro.chem. Int. 1999, 35, 11–17.
41. J.R Leach, and A.M.Muenster J. Nutr., 1962, 78, 51–56.
42. C. Paluszkiewicz, A. Slosarczyk, D. Pijocha M. Sitarz, M. Bućko, A. Zima, A. Chróścicka, and M. L.Szumieł, J. Molecular. Structure., 2010, 976, 301-309.
43. J. Brozmanová, D. Mániková, V. Vcková, and M. Chovanec, Arch. Toxicol., 2010, 84, 919-938.
44. P.A. Tran, L. Sarin, R.H. Hurt, and T.J.Webster J. Biomed. Mater. Res. Part A., 2010, 93,1417-1428.
45. M.P Rayman. Lancet, 2000, 356, 233-241.
46. M.N. Alarcon and C.L. Martinez Sci. Total. Environ., 2000, 47, 295-308.
47. G.F. Combs, and W.P.Gray Pharmacol. Therapeut., 1998, 79, 179-192.
48. C. Jiang, W.Q. Jiang, H. Ganther, and L.X. Lu Mol. Carcinogen. 1999, 26, 213-225.
49. P. Tran, and T.J.Webster Int. J. Nanomed., 2008, 3, 391-396.
50. P.A. Tran, L. Sarin, R.H. Hurt, and T.J.Webster Int. J. Nanomed., 2010, 5, 351-358.
51. J. Kolmas , E. Oledzka , M. Sobczak , and G. N. Jawecki , Mater. Sci. Eng. C., 2014, 39, 134–142.
52. V. Perla, and T.J.Webster J. Biomed Mater Res A., 2005, 75, 356–364.
53. X. F. Xiao, R. F. Liu and Y. Z. Zheng, Surf. Coat. Technol., 2006, 200, 4406–4413.
54. Y. Song, S. Zhang, J. Li, C. Zhao and X. Zhang, Acta Biomater., 2010, 6, 1736–1742.
55. Y. W. Song, D. Y. Shan and E. H. Han, Mater. Lett., 2008, 62, 3276–3279.
56. J. Wang, Y. Chao, Q. Wan, Z. Zhu and H. Yu, Acta Biomater., 2009, 5 (5), 1798-1807
57. W.S. Hummers, and R.E.Offeman J.Am .Chem .Soc., 1958, 80, 1339–1340.